Terahertz-Induced Field-Free Orientation of Rotationally Excited Molecules

K. N. Egodapitiya, Sha Li, and R. R. Jones
Department of Physics, University of Virginia, Charlottesville, Virginia 22904-4714, USA
(Received 9 December 2013; published 12 March 2014)

We have used picosecond THz pulses to induce transient field-free orientation of OCS molecules. Coherent optical Raman excitation prepares the molecules in rotational superposition states prior to THz irradiation, substantially enhancing the degree of orientation. The time-dependent alignment and orientation are characterized via Coulomb explosion in an intense probe laser. The degree of OCS orientation is an order of magnitude larger than previously observed following THz irradiation and is achieved with a significantly smaller THz field.The field-free orientation level is comparable to that generated using pulsed, two-color laser fields but is obtained with negligible target ionization.

DOI: 10.1103/PhysRevLett.112.103002 PACS numbers: 33.80.Rv, 32.80.Qk, 33.80.Wz, 42.50.Hz

Manipulation of the angular degrees of freedom of gas phase molecules has received substantial attention in the last few decades [1–22], driven in part by the desire to eliminate the uncertainties and averaging that are inherent in measurements involving molecules with random angular distributions. Additionally, the availability of aligned or oriented samples might enable efficient control of chemical, surface, or photoreactions whose rates depend on molecular orientation relative to various laboratory-fixed parameters, including propagation, surface, or polarization directions. Aligned molecules possess well-defined angle(s) between body-and laboratory-fixed axes while oriented molecules also have a polarity (e.g., permanent dipole moment) in a specific direction in the lab frame.

In general, it is considerably more difficult to create highly oriented, as compared to well-aligned, targets. That said, several techniques have successfully produced oriented samples [1–7,9–17]. In most cases, static or optical fields must be applied throughout an experiment in order to maintain the desired orientation [4–7,9–16]. Unfortunately, these fields can influence the primary measurements of interest if they alter the molecular structure, induce subsidiary dynamics, or complicate the detection of reaction products, e.g., low energy electrons. In addition, some methods require molecular beam propagation through a spatially extended field region to achieve rotational state selection [4,12–15]. This can limit sample density, precluding the use of these techniques in some experiments, e.g., those involving high harmonic generation [3,23,24].

Methods for achieving field-free orientation also exist [1–3,8,17]. As with field-free alignment, this orientation is transient and results from the dynamic evolution of a rotational wave packet created during the exposure of the sample to one or more pulsed electromagnetic fields. Transient orientation can be readily exploited in experiments involving short-pulse laser interactions where a well-defined orientation of the molecules in the lab frame is only required during a specific, brief time interval. To date, the degree of orientation achieved with field-free methods [1–3] is modest in comparison with that attainable using state-selective techniques [14,15]. Moreover, the two-color approach [2,3] (which has been the most effective), requires high intensities, potentially (or necessarily) causing substantial ionization [3] and electronic or vibronic excitation that may be unacceptable in some applications. Here, we describe measurements that demonstrate that coherent optical preparation of a rotational wave packet can enhance, by an order of magnitude, the level of field-free orientation induced by a THz pulse [1] without the need for intense, ionizing laser pulses.

In contrast to optical orientation techniques that rely on rotational excitation of mixed parity wave packets through hyper-Raman transitions [2] or ionization depletion [3], THz orientation involves direct rotational excitation enabled by the interaction of the molecule's permanent dipole moment with a carrier-envelope-phase locked field [1,8,17,25,26]. For most molecules, with fundamental rotational transitions at frequencies of tens of GHz or less (e.g., $B_{\mathrm{OCS}} = 6.09$ GHz), the low-frequency cutoff in single-cycle and laboratory available "half-cycle" THz pulses renders them quite inefficient in driving transitions between the low-lying rotational states that are populated in a cold sample. At higher temperatures, molecules in higher rotational states are populated and can be efficiently excited to neighboring levels by a THz pulse. However, as with transient alignment, the achievable coherence is quite low, resulting in very weak orientation even with field strengths of several hundred kV/cm [1]. As an alternative, we utilize Raman redistribution in a short optical pulse to coherently prepare molecules in highly excited rotational states prior to THz exposure [25,26]. The excitation improves the overlap of the THz and rotational spectra and, when the THz pulse is properly timed, interference [27] suppresses the excitation of oppositely oriented components in the ensemble, substantially increasing the net orientation.

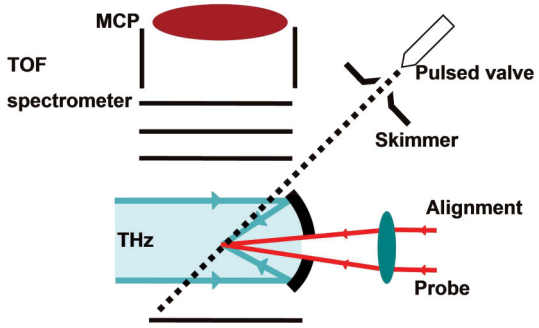

FIG. 1 (color online). Schematic of the transient orientation experiment.

In the experiment (Fig. 1), OCS molecules are first exposed to a short laser pulse whose intensity is sufficient to induce a significant level of transient molecular alignment but negligible ionization. The rotationally excited molecules coherently evolve for a time, Δt_1, and are not optimally aligned (or antialigned) when they are exposed to a single-cycle THz pulse. The THz field directly drives transitions between rotational states, creating a mixed-parity wave packet whose field-free evolution exhibits periodic orientation. The angular distribution of ion fragments produced via Coulomb explosion in an intense, time-delayed probe laser is used to measure the time-dependent alignment or orientation of the sample.

A beam of rotationally cold ($T \simeq 2$ K) OCS molecules in He is produced in a supersonic expansion originating from a pulsed, Even-Lavie (EL) valve [28,29]. The 800 nm alignment and probe laser pulses are created in a 2 mJ, 35 fs, 15 Hz, multipass Ti:sapphire amplifier. Approximately 40% of the output energy is directed into the alignment pulse, and the remainder is used for the probe. The alignment and probe beams are focused by a 250 mm focal length lens, through a 5 mm hole in a THz-focusing mirror, into the perpendicularly propagating OCS beam. The alignment beam is apertured prior to the lens to increase the focal spot size. This ensures that all molecules sampled by the probe experience nearly the same alignment laser intensity. Propagation through glass increases the alignment pulse duration to ~60 fs, so that it causes negligible ionization. The intensities of the alignment and probe lasers are 3×10^{13} W/cm^2 and 1×10^{15} W/cm^2, respectively. An extraction field (~400 V/cm) applied to the interaction region pushes ions formed by the probe pulse toward a microchannel plate (MCP) detector. The degree of orientation observed is independent of whether the field is switched on after the probe pulse or is applied throughout the experiment. The OCS and He pressures are adjusted to minimize the OCS rotational temperature while producing no signature of clusters in the ion TOF spectrum.

The THz pulses are produced via optical rectification of 20 mJ, 100 fs, 790 nm laser pulses in $LiNbO_3$, using a tilted-pulse-front pumping scheme [30,31]. The 790 nm laser pulses are generated in a 15 Hz regenerative amplifier. After leaving the $LiNbO_3$ crystal, the THz radiation is collected by a 75 mm diameter off-axis paraboloid. The THz beam enters the vacuum chamber through a Teflon window, counterpropagates with the alignment and probe laser beams, and passes through the spectrometer with low intensity (diameter ≈50 mm). A 50 mm focal length spherical mirror retroreflects and focuses the THz beam to a 3.5 mm diameter spot in the interaction region. Using a pyroelectric energy meter and *in situ* THz streaking [32] of photoelectrons from OCS, we determine that the THz field has the form of a single-cycle sine wave with a duration of 2 ps, a bandwidth and central frequency of approximately 0.25 THz, and a peak field of ~120 kV/cm. The Rayleigh length of the THz focus is 25 mm, so the Gouy phase variation is essentially negligible over the 2 mm diameter of the OCS beam it crosses. The linear polarizations of the THz and alignment laser beams are parallel to the vertical spectrometer axis.

The time-dependent alignment or orientation of the OCS molecules is characterized using the TOF distribution of S^{3+} ion fragments that are produced as Coulomb explosion by-products following enhanced ionization in the intense probe. Efficient enhanced ionization requires the molecular axis to be nearly parallel to the probe laser polarization [33], so highly charged species such as S^{3+} are ejected via Coulomb explosion in a narrow cone about the probe polarization [34,35]. With a circularly polarized probe, OCS molecules which lie in the vertical polarization plane are representative of the entire ensemble, and these are converted to S^{3+} ions with uniform probability. All ions eventually reach the detector due to the extraction field, but those ejected toward (away) from the detector arrive sooner (later) [36]. Accordingly, the S^{3+} TOF distribution reflects the molecular angular distribution during the probe pulse [36]. Of the fragments we observe, the S^{3+} ions are best suited for the probe measurements because: they are highly directional and are only produced via enhanced ionization at our probe intensities; their large kinetic energy release makes it easier to distinguish fragments ejected in different directions; and their TOF distribution is not contaminated by other species with identical, or similar, charge to mass ratios.

The black curve in the Fig. 2 inset shows a portion of the ion TOF spectrum for unaligned and unoriented OCS molecules. The green curve shows the analogous spectrum obtained with the probe positioned 40 ps after an $I \sim 3 \times 10^{13}$ W/cm^2 alignment pulse, i.e., during a rotational half revival. The bimodal structure of the S^{3+} signal in the green trace clearly reflects the molecular alignment along the spectrometer axis, with a decrease in the number of ions ejected in, or near, the horizontal plane and a corresponding increase in those ejected directly toward or away from the detector. We obtain a measure of alignment [36] by integrating the S^{3+} ion signal appearing in three

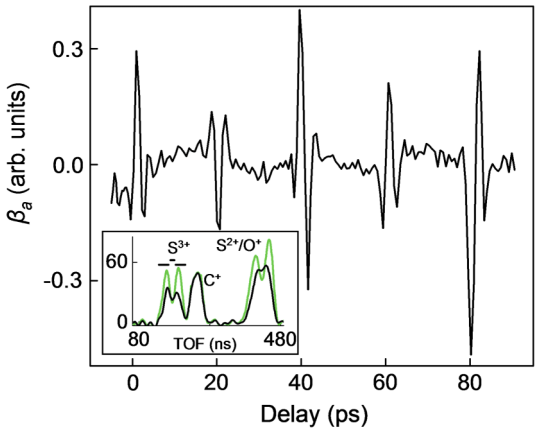

FIG. 2 (color online). Alignment parameter β_a (averaged over 30 laser shots) vs alignment-probe delay. Inset: Partial ion TOF spectrum produced by a circularly polarized probe laser, for unaligned (black) and aligned (green) molecules. In the green curve, the alignment-probe delay is 40 ps and the TOF signal reflects the rotational angular distribution of OCS molecules which are preferentially aligned along the spectrometer axis. The horizontal bars above the S^{3+} ion peaks depict the time bins used to measure β_a and β_o.

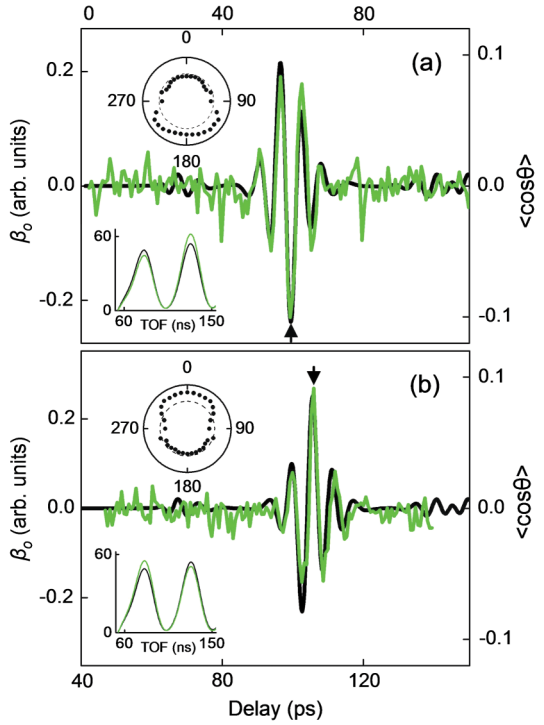

FIG. 3 (color online). Measured orientation parameter β_o (green) and calculated $\langle \cos\theta \rangle$ (black) vs alignment-probe delay for (a) $\Delta t_1 = 22$ ps and (b) $\Delta t_1 = 60$ ps. Δt_1 is defined as the interval between the temporal centers of the alignment and THz pulses. Upper insets: Tomographic reconstruction of the rotational probability distribution for S atoms in OCS, obtained at the delays marked by the arrows in the main figures. Black dots are the measured probability density vs probe polarization angle θ relative to the vertical. Lower insets: S^{3+} TOF signal for unoriented (black) and oriented (green) molecules obtained under the same conditions used to measure the distributions in the upper insets.

time bins (Fig. 2 inset) and calculating the normalized difference, $\beta_a = [I_1 + I_2 - 2I_3]/[I_1 + I_2 + 2I_3]$. Here I_1, I_2, and I_3 are integrated signals in the early, late, and middle time bins, respectively. Figure 2 shows the alignment parameter β_a (with a constant background subtracted) as a function of the alignment-probe delay. The alignment revival structure matches that predicted for bare OCS, providing additional evidence that enhanced ionization of OCS molecules (not He_n + OCS clusters [37]) is the predominant source of S^{3+} ions in our experiment. The Fourier transform of $\beta_a(t)$ reveals the spectrum of the coherently excited rotational states [36]. The spectrum peaks at $J = 10$ and extends to $J = 16$, where the frequencies of the $|J\rangle \rightarrow |J+1\rangle$ transitions are 0.13 and 0.21 THz, respectively. Thus, the relevant transitions for creating mixed-parity orienting wave packets fall within the bandwidth of the THz pulse.

If preferential orientation were established along the vertical axis, a greater number of S^{3+} ions would be ejected toward (or away from) the detector, depending on the sign of the orientation. We use a vertically polarized probe laser and an orientation parameter $\beta_o = (I_1 - I_2)/(I_1 + I_2)$ to search for time-dependent orientation. Aside from small transients, caused by statistical differences in the number of ion counts in the early and late time bins (which can be more prevalent at alignment revivals times), $\beta_o = 0$ in the absence of the THz pulse. This indicates that, as expected, no preferential orientation is produced by the alignment pulse alone. In contrast, the application of the THz pulse after the alignment laser leads to a substantial degree of time-dependent orientation.

Figure 3 shows our principal results. The solid green curves in Figs. 3(a) and 3(b) show the measured values of β_o as a function of the alignment-probe delay, with the THz pulse positioned at $\Delta t_1 = 22$ and 60 ps after the alignment pulse, near the 1/4 and 3/4 alignment revivals, respectively. In both cases, a clear oscillation in β_o is observed at $\Delta t_2 \sim 40$ ps after the THz pulse, reflecting a modulation in the preferential orientation. Δt_2 is defined as the interval between the temporal centers of the THz and probe pulses. The coherent rotational preparation of the ensemble is critical for observing orientation within the signal to noise ratio for the experiment. No orientation is observed at $\Delta t_2 \sim 40$ ps if the alignment laser is blocked. Moreover, with or without the alignment laser, no orientation is observed at the times predicted for molecular orientation by the THz pulse alone [8], i.e., near $\Delta t_2 = 0$, τ.

The orientation enhancement near $\Delta t_2 = \tau/2 \simeq 40$ ps is the result of coherent rotational excitation during the alignment pulse [38]. Consider a molecule in a single rotational state $|J \neq 0\rangle$. The application of a weak,

broadband THz pulse creates a coherent rotational superposition whose principal components, $|J\rangle$, $|J+1\rangle$, and $|J-1\rangle$, have phases which evolve in proportion to their energies. Transient orientation occurs when the even and odd parity eigenstate constituents interfere, enhancing the rotational wave function at positive (negative) values of z while suppressing it at negative (positive) z. Because the excitation of $|J+1\rangle$ ($|J-1\rangle$) from $|J\rangle$ involves the absorption (emission) of a THz photon, the excitation amplitudes have different phases. Accordingly, when Δt_2 is near an integer multiple of τ, the Δt_2 values for which the $|J\rangle + |J+1\rangle$ interference gives the maximum probability amplitude for positive z coincide with the Δt_2 values for which the $|J\rangle + |J-1\rangle$ interference gives maximum probability amplitude for negative z. In general, this cancellation of the two interference terms is not complete because the excitation amplitudes to $|J+1\rangle$ and $|J-1\rangle$ are not identical, so a weak residual orientation results. Conversely, when Δt_2 is near a half-integer multiple of τ, the two interference terms have the same sign, producing the maximum degree of orientation.

Interestingly, the sign of the orientation induced at half revivals depends on the parity of the initial state $|J\rangle$, but the sign of the orientation near full revivals is J independent [39]. Thus, when starting from an incoherent rotational ensemble at nonzero temperature (where roughly half of the molecules are in states with even J and the others have odd J) the net orientation near half-revival times is zero, but a small degree of orientation is achieved when Δt_2 is near 0 or a full revival. As described below, by properly adjusting Δt_1, we can suppress the creation of mixed-parity wave packets from either the even or the odd initial states, thereby eliminating the destructive interference, which destroys the net orientation when Δt_2 is near a half revival.

The alignment pulse coherently excites, via rotational Raman transitions, ladders of like-parity rotational levels from each thermally populated initial state. This coherent population redistribution improves the efficiency of the subsequent THz excitation probability since, for higher lying states, the transition frequencies to neighboring levels fall closer to the peak of the THz spectrum. Moreover, because the Raman redistribution from each initial state is coherent, in a given ladder, the THz transition amplitudes for $|J+1\rangle \rightarrow |J\rangle$ and $|J-1\rangle \rightarrow |J\rangle$ interfere. For even parity ladders, the interference is predominantly constructive (destructive) for $\Delta t_1 \simeq \tau/4, 5\tau/4, \ldots$ ($3\tau/4, 7\tau/4, \ldots$). The interference condition is opposite for odd parity ladders. Hence, for $\Delta t_1 \simeq \tau/4$, molecules in even parity ladders are converted to mixed parity wave packets (which exhibit strong orientation at a probe delay $\Delta t_2 \simeq \tau/2$), whereas those in odd parity ladders are not. Since only initial states of even parity contribute to the orientation, there is no net cancellation in the strong ensemble orientation at $\Delta t_2 \simeq \tau/2$. Conversely, for $\Delta t_1 \simeq 3\tau/4$, only odd initial states contribute to the strong orientation observed at $\Delta t_2 \sim \tau/2$. These arguments (fully supported by numerical simulations) predict that the peak orientation levels obtained for $\Delta t_1 \simeq \tau/4$ and $3\tau/4$ should have opposite signs, because the primary contributors to the ensemble orientation are initially even and odd levels, respectively. Inspection of Fig. 3 shows that this is, indeed, the case.

We use tomographic reconstruction of the rotational probability distribution to quantify the degree of orientation in the experiment (Fig. 3). The probe and THz delays are fixed and the S^{3+} TOF distribution is measured with a linearly polarized probe as a function of its polarization angle θ relative to vertical. For each θ, an S^{3+} ion yield ratio (with:without the alignment + THz pulses) is computed for both the forward and backward ion peaks. These ratios give the probabilities for finding the S atom in the forward or backward direction along the laser polarization axis. The ratio measurements obtained at different θ are combined to generate the rotational probability distributions. From these, we determine the ensemble averaged moments $\langle \cos\theta \rangle = -0.10$ and 0.08 at the delays marked by the arrows in Figs. 3(a) and 3(b), respectively. This degree of field-free orientation is comparable to that observed with two-color schemes [2,3], but is obtained with negligible sample ionization.

Figures 3(a) and 3(b) also show $\langle \cos\theta \rangle$ obtained by numerically integrating the time-dependent Schrödinger equation for an ensemble of rigid rotors with rotational constant B_{OCS} at a temperature T. Rotational excitation occurs via the combined laser and THz interactions, $U(\theta, t) = -1/4\langle F^2(t)\rangle \alpha_{\mathrm{OCS}} \cos^2\theta + F_{\mathrm{THz}}(t) d_{\mathrm{OCS}} \cos\theta$, where $\langle F^2(t)\rangle$ is the time averaged square of the alignment field, $F_{\mathrm{THz}}(t)$ is the THz field, and $\alpha_{\mathrm{OCS}} = 31$ a.u. and $d_{\mathrm{OCS}} = 0.28$ a.u. are the polarizability anisotropy and permanent dipole moment, respectively. Aside from the THz interaction term, the calculations proceed identically to those described previously [36], and enable the determination of the ensemble averaged, delay-dependent, angular probability distribution. We adjust the peak alignment intensity I and temperature T to obtain the best agreement between the calculated time dependence of $\langle \cos\theta \rangle$ and the measured time dependence of β_o. The period of the large oscillations in $\langle \cos\theta \rangle$ is determined by I, whereas T sets the width of the temporal envelope of those oscillations. The best simultaneous fits to the data in Figs. 3(a) and 3(b) are obtained with $I = 2.8 \times 10^{13}$ W/cm^2 and $T = 2$ K. This intensity is in agreement with direct measurements and the temperature is reasonable for the *EL* valve. With I and T fixed, the THz field determines the maximum degree of orientation. We find that peak THz fields of 24 and 29 kV/cm reproduce the measured ensemble-averaged moments, $\langle \cos\theta \rangle = -0.10$ and 0.08 [40].

In conclusion, we have used THz pulses to induce field-free orientation of OCS molecules. Substantial orientation enhancement is achieved through coherent rotational

excitation prior to THz exposure. The technique results in negligible electronic excitation or ionization and is readily applicable to measurements aimed at investigating and controlling molecular dynamics using ultrafast lasers. The degree of transient orientation is an order of magnitude larger than that observed previously with THz excitation alone in molecules with small (OCS [1]) and large (HBr [17]) rotational constants. For OCS, the higher degree of orientation is achieved with a THz field that is an order of magnitude smaller. We have generated THz fields in excess of 420 kV/cm on target in vacuum using a different focusing geometry [41]. Thus, it should be straightforward to substantially improve the achievable degree of transient orientation or reproduce it at kHz repetition rates using sub-mJ optical pump energies.

It is a pleasure to acknowledge helpful conversations with H. Stapelfeldt, S. Fleischer, K. Nelson, and V. Kumarappan. This work is supported by the Chemical Sciences, Geosciences, and Biosciences Division of the Office of Basic Energy Sciences, U.S. Department of Energy.

[1] S. Fleischer, Y. Zhou, R. W. Field, and K. A. Nelson, Phys. Rev. Lett. **107**, 163603 (2011).
[2] S. De, I. Znakovskaya, D. Ray, F. Anis, N. G. Johnson, I. A. Bocharova, M. Magrakvelidze, B. D. Esry, C. L. Cocke, I. V. Litvinyuk, and M. F. Kling, Phys. Rev. Lett. **103**, 153002 (2009).
[3] E. Frumker, C. T. Hebeisen, N. Kajumba, J. B. Bertrand, H. J. Worner, M. Spanner, D. M. Villeneuve, A. Naumov, and P. B. Corkum, Phys. Rev. Lett. **109**, 113901 (2012).
[4] D. H. Parker and R. B. Bernstein, Annu. Rev. Phys. Chem. **40**, 561 (1989).
[5] H. J. Loesch and A. Remscheid, J. Chem. Phys. **93**, 4779 (1990).
[6] B. Friedrich and D. Herschbach, Nature (London) **353**, 412 (1991).
[7] K. Nauta, D. T. Moore, and R. E. Miller, Faraday Discuss. **113**, 261 (1999).
[8] M. Machholm and N. E. Henriksen, Phys. Rev. Lett. **87**, 193001 (2001).
[9] H. Sakai, S. Minemoto, H. Nanjo, H. Tanji, and T. Suzuki, Phys. Rev. Lett. **90**, 083001 (2003).
[10] U. Buck and M. Farnik, Int. Rev. Phys. Chem. **25**, 583 (2006).
[11] A. Goban, S. Minemoto, and H. Sakai, Phys. Rev. Lett. **101**, 013001 (2008).
[12] I. Nevo, L. Holmegaard, J. H. Nielsen, J. L. Hansen, H. Stapelfeldt, F. Filsinger, G. Meijer, and J. Kupper, Phys. Chem. Chem. Phys. **11**, 9912 (2009).
[13] L. Holmegaard, J. H. Nielsen, I. Nevo, H. Stapelfeldt, F. Filsinger, J. Kupper, and G. Meijer, Phys. Rev. Lett. **102**, 023001 (2009).
[14] O. Ghafur, A. Rouzee, A. Gijsbertsen, W. K. Siu, S. Stolte, and M. J. J. Vrakking, Nat. Phys. **5**, 289 (2009).
[15] L. Holmegaard, J. L. Hansen, L. Kalhoj, S. L. Kragh, H. Stapelfeldt, F. Filsinger, J. Kupper, G. Meijer, D. Dimitrovski, M. Abu-samha, C. P. J. Martiny, and L. B. Madsen, Nat. Phys. **6**, 428 (2010).
[16] K. Oda, M. Hita, S. Minemoto, and H. Sakai, Phys. Rev. Lett. **104**, 213901 (2010).
[17] K. Kitano, N. Ishii, N. Kanda, Y. Matsumoto, T. Kanai, M. Kuwata-Gonokami, and J. Itatani, Phys. Rev. A **88**, 061405(R) (2013).
[18] T. Seideman, Phys. Rev. Lett. **83**, 4971 (1999).
[19] F. Rosca-Pruna and M. J. J. Vrakking, Phys. Rev. Lett. **87**, 153902 (2001).
[20] H. Stapelfeldt and T. Seidemann, Rev. Mod. Phys. **75**, 543 (2003), and references therein.
[21] J. L. Hansen, H. Stapelfeldt, D. Dimitrovski, M. Abu-samha, C. P. J. Martiny, and L. B. Madsen, Phys. Rev. Lett. **106**, 073001 (2011).
[22] P. Hockett, C. Z. Bisgaard, O. J. Clarkin and A. Stolow, Nat. Phys. **7**, 612 (2011).
[23] E. Frumker, N. Kajumba, J. B. Bertrand, H. J. Worner, C. T. Hebeisen, P. Hockett, M. Spanner, S. Patchkovskii, G. G. Paulus, D. M. Villeneuve, A. Naumov, and P. B. Corkum, Phys. Rev. Lett. **109**, 233904 (2012).
[24] P. M. Kraus, A. Rupenyan, and H. J. Worner, Phys. Rev. Lett. **109**, 233903 (2012).
[25] K. Kitano, N. Ishii, and J. Itatani, Phys. Rev. A **84**, 053408 (2011).
[26] C.-C. Shu and N. E. Henriksen, Phys. Rev. A **87**, 013408 (2013).
[27] K. F. Lee, D. M. Villeneuve, P. B. Corkum, and E. A. Shapiro, Phys. Rev. Lett. **93**, 233601 (2004).
[28] U. Even, J. Jortner, D. Noy, N. Lavie, and C. Cossart-Magos, J. Chem. Phys. **112**, 8068 (2000).
[29] 400 ppm OCS is expanded in 70 atm of He into a 10^{-8} Torr vacuum. The valve-opening time on our *EL* controller is 15.7 μs, but the precise pulse duration has not been measured.
[30] J. Hebling, K.-L. Yeh, M. C. Hoffmann, B. Bartal, and K. A. Nelson, J. Opt. Soc. Am. B **25**, B6 (2008).
[31] H. Hirori, A. Doi, F. Blanchard, and K. Tanaka, Appl. Phys. Lett. **98**, 091106 (2011).
[32] U. Fruhling *et al.*, Nat. Photonics **3**, 523 (2009).
[33] T. Seideman, M. Yu. Ivanov, and P. B. Corkum, Phys. Rev. Lett. **75**, 2819 (1995).
[34] D. T. Strickland, Y. Beaudoin, P. Dietrich, and P. B. Corkum, Phys. Rev. Lett. **68**, 2755 (1992).
[35] K. J. Betsch, D. W. Pinkham, and R. R. Jones, Phys. Rev. Lett. **105**, 223002 (2010).
[36] D. Pinkham and R. R. Jones, Phys. Rev. A **72**, 023418 (2005).
[37] F. Paesani, A. Viel, F. A. Gianturco, and K. B. Whaley, Phys. Rev. Lett. **90**, 073401 (2003), and references therein.
[38] The enhancement mechanism is distinct from that previously proposed [42] for improving half-cycle pulse induced orientation via molecular antialignment.
[39] V. Kumarappan (private communication).
[40] These fields are four times smaller than expected but are consistent with no detected orientation in the absence of the alignment pulse.
[41] S. Li and R. R. Jones (to be published).
[42] E. Gershnabel, I. Sh. Averbukh, and R. J. Gordon, Phys. Rev. A **73**, 061401 (2006).